Journal of Physics: Conference Series **2362** (2022) 012018 doi:10.1088/1742-6596/2362/1/012018

Seabed bathymetry and friction modeling in MoorDyn

Stein Housner[1], Ericka Lozon[1], Bruce Martin[2], Dorian Brefort[2] and Matthew Hall[1]

[1] National Renewable Energy Laboratory, Golden, Colorado, USA
[2] Principle Power Inc., Emeryville, California, USA

E-mail: Stein.Housner@nrel.gov

Abstract. This paper presents the implementation and verification of a seabed bathymetry feature and seabed friction feature to the open-source, lumped-mass mooring system dynamics modeler, MoorDyn, which is part of the National Renewable Energy Laboratory's aero-hydro-servo-elastic simulation tool, OpenFAST. Variations in seabed slope, as well as the frictional effects of mooring lines moving along the seabed, will affect the mooring line tensions of a floating platform and the consequent platform response. These new features are especially relevant for modeling mooring systems in deep-water coastal areas where seabed depth can change significantly over an entire mooring footprint. The bathymetry feature models the seabed as a rectangular grid of variable water depths in place of the existing, uniform water depth in MoorDyn. The friction force is primarily represented as a Coulombic friction force, or the product of a kinetic friction coefficient and the seabed contact normal force, with the ability to differentiate between transverse and axial motion of a line node on the seabed in any bathymetry grid. These capabilities were tested by running MoorDyn and OpenFAST simulations over a variety of seabed and environmental conditions; the resulting fairlead tensions, node tensions, and mooring line kinematics were verified against equivalent OrcaFlex simulations. The results match closely, meaning the features are verified, which will increase the overall fidelity of OpenFAST and FAST.Farm simulations.

1. Introduction

The continued development and cost reduction of marine renewable energy devices, especially floating offshore wind turbines (FOWTs), is dependent on the validity of their modeling tools. The validity of these tools depends on how well they incorporate the real-world physical aspects in predicting the floating system's behavior. There are many physical aspects that need to be considered for a FOWT, such as aerodynamics, hydrodynamics, and environmental conditions, but the one relevant to this paper is the mooring dynamics. At a minimum, mooring modeling tools need to calculate the mooring line tensions in a mooring system based on the mooring configuration, the properties of the mooring components, and the system motions. To increase the fidelity of the model and accurately predict the desired outputs, other real-world physical aspects should be included in these calculations. Two such considerations, which will be the focus of this paper, are the seabed bathymetry and the seabed friction effects on a mooring system.

With growing interest in floating offshore wind energy development in places like the U.S. West Coast where there are high gradients in seabed depth, the effects of seabed bathymetry and friction on the mooring system and platform response are becoming more important to accurately model. To date, some proprietary mooring dynamics tools model seabed bathymetry, but the effects of bathymetry on the mooring system have not been investigated thoroughly. Two proprietary mooring dynamics tools, ProteusDS [1] and OrcaFlex [2], include seabed bathymetry models that include options for a flat, sloped, or three-dimensional bathymetry profile. MAP, an open-source program used to model multisegmented, quasi-static mooring systems in OpenFAST, however, is unable to model three-dimensional bathymetries [3]. Various mooring studies note that bathymetry can be a parameter in a mooring system, but do not include any variations of seabed depth in their work [4].

The effects of seabed friction on a mooring system have previously been represented using various friction models. Azcona et al. [5] developed a new mooring and anchoring code, which models friction on a flat seabed using horizontal springs to counteract the applied load on a node, while considering the axial and transverse directions independently. Like [5], most friction models utilize a Coulomb friction model, which calculates the friction force as the product of a friction coefficient and the seabed contact normal force. Lee et al. [6] introduced a modified Coulomb friction model, which calculates the friction coefficient as a function of the node velocity but is unable to model sticking of line nodes, resulting in slow slippage. To account for these deficiencies, Choi and Yoo [7] developed a friction model that accounts for node slippage using a spring-damper system. Liu and Bergdahl [8] calculated the friction force in the time domain as either a Coulombic friction force or a force proportional to the node velocity, depending on the individual node velocity. OrcaFlex has the option to use two seabed friction models: an elastic model and a nonlinear soil model [2]. The elastic model represents the seabed as a simple elastic linear or nonlinear spring in both the axial and transverse directions. The nonlinear soil model represents the axial friction nonlinearly to model nonlinear behaviors like suction effects. MAP uses a cable-seabed friction coefficient in the mooring analytic equations to model seabed friction but is unable to account for friction in a dynamics analysis [3].

MoorDyn, the mooring dynamics module that is part of the National Renewable Energy Laboratory's coupled aero-hydro-servo-elastic simulation tool OpenFAST, has been shown to accurately predict the mooring line fairlead tensions and platform response in uncoupled and coupled simulations under generic laboratory conditions [9]. It has also previously undergone versions of seabed friction implementation. Hall [10] initially attempted a simple saturated damping approach to model friction in MoorDyn. Devries and Hall [11] expanded on the previous study and implemented two different friction models into the MoorDyn-C version and compared the differences between the two models and the no-friction case. MoorDyn assumes a completely flat seabed over the entire mooring footprint, allowing for no variation in seabed bathymetry, which could have led to inaccurate results when modeling irregular seabeds. No open-source mooring dynamics model has incorporated both of these seabed considerations before.

In this paper, proposed seabed bathymetry and seabed friction models are discussed and then implemented into the MoorDyn source code. The models are verified by comparing MoorDyn and OpenFAST simulations to equivalent OrcaFlex simulations using three different mooring systems and four different seabed bathymetry conditions. Under these conditions, the fairlead tensions, node tensions, and mooring line kinematics are compared between the two models to assess how well these new features can accurately predict the mooring system's behavior.

2. Methodology

The seabed bathymetry feature and the seabed friction feature in MoorDyn are implemented using the latest development versions of MoorDyn version 2 and OpenFAST version 3.0.0. The bathymetry implementation involves an additional input file of a bathymetry grid, which will be used with a bilinear interpolation algorithm to determine the local seabed depth and slope of mooring line nodes on the seabed and anchor points. The friction implementation involves the addition of a friction force on the line nodes resting on or below the seabed using a variation of a Coulombic friction model with distinctions between the transverse and axial directions of the mooring line nodes.

2.1. Bathymetry

The seabed bathymetry feature allows for a desired bathymetry to be mapped to a bathymetric surface grid of any rectangular discretization to characterize the changes in water depth throughout the footprint of a mooring system. The bathymetry grid contains the layout of local seabed depths at specific x- and y-locations across the mooring footprint. Figure 1 shows an example bathymetry grid (Figure 1a) and grid panel (Figure 1b) with its unit normal vector.

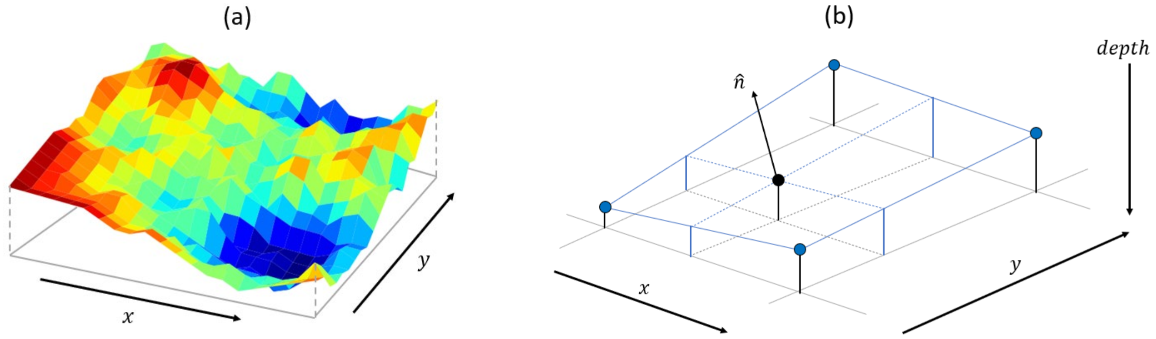

Figure 1. Example bathymetry grid (a) and grid panel (b) with unit normal vector.

A bathymetry grid surface can be a completely horizontal plane, a continuous sloped plane in any direction, or be user-defined by any three-dimensional surface. Once imported and created, MoorDyn then references this bathymetry grid with the x and y location of any point of interest that lies on the seabed in the mooring system and uses bilinear interpolation to determine its local seabed depth inside the bathymetry grid cell.

2.2. Friction

The seabed friction model that was implemented into MoorDyn is a saturated damping friction model. It is derived from the Coulombic friction model that models a kinetic friction force as the product of a kinetic friction coefficient and the seabed contact normal force and does not include any static friction effects (Figure 2a). However, the standard Coulombic friction model always applies the friction force to an object in contact with the seabed, which is not conducive for numerical simulations, like MoorDyn, due to the discontinuity that arises when the sign of the friction force abruptly flips when velocity changes direction. To avoid this instability, the Coulombic friction model is altered to produce the saturated damping model. The new model calculates the friction force as a function of the object's velocity to give a continuous "ramp-up" section in the lower velocity region for the static friction force, and then models a kinetic friction force for all other velocities (Figure 2b). The friction force is calculated with respect to velocity because it is easier to determine whether an object is sliding based on its velocity rather than on its position, which would require knowledge of previous positions.

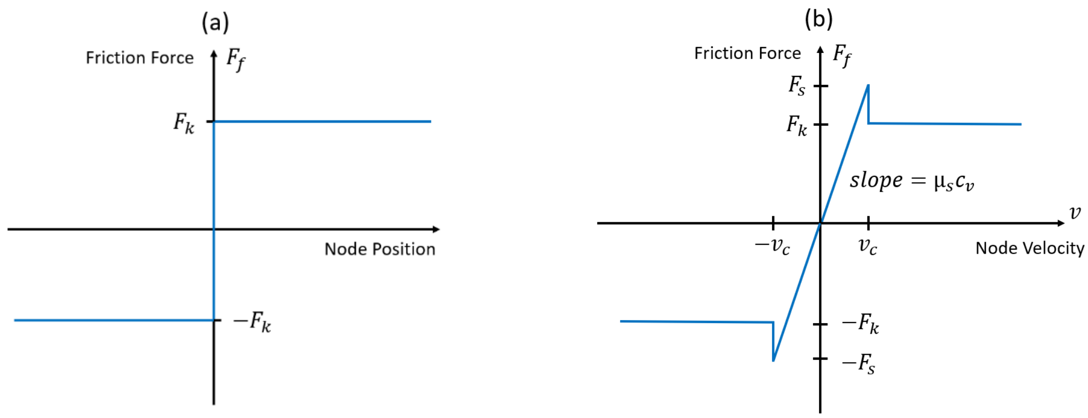

Figure 2. Coulombic (a) and saturated damping (b) friction model depictions.

The kinetic friction force (F_k) (the constant horizontal line in Figure 2a and Figure 2b) is the product of the kinetic friction coefficient (μ_k) and the seabed contact normal force (F_n), where the seabed contact normal force can have components in the x, y, and z directions due to any sloped bathymetry, as shown in equation (1):

$$\boldsymbol{F_k} = \mu_k \boldsymbol{F_n} \tag{1}$$

The nuanced part of the saturated damping model is the friction force slope in the low-velocity region. The reason this slope exists is to avoid the discontinuity in regular Coulombic friction models. To numerically model the friction force, an arbitrary ramp-up velocity (v_c) is set as the velocity at which the static friction force is achieved. Any velocity above this threshold yields the kinetic friction force and any velocity below this threshold yields a fraction of the static friction force. Normally, the fraction would depend on the magnitude of the applied load on the object in the opposite direction. However, because the friction model is a function of node velocity, the fraction will depend on the arbitrary ramp-up velocity threshold and the node velocity. In essence, this friction force ramp-up can be portrayed as a mooring line node creeping along the seabed until the velocity threshold is reached and the full kinetic friction force is applied. Ideally, the line node would be held still by the static friction force until the applied force overcomes the static friction force, resulting in the kinetic friction force as the line node starts to move. This velocity threshold should be as close to zero as possible to ensure that the kinetic friction force is only applied to line nodes in motion.

Like the kinetic friction force, the static friction force (F_s) is the product of the static friction coefficient (μ_s) and the seabed contact normal force (F_n), as shown in equation (2):

$$\boldsymbol{F_s} = \mu_s \boldsymbol{F_n} \tag{2}$$

The slope of the ramp-up curve of the saturated damping friction model can be shown using Figure 2b as the static friction force (F_s) over the ramp-up break velocity (v_c). Dividing the static friction force in equation (2) by v_c and recognizing that a force-over-velocity term can also be considered a damping term, the slope of the ramp-up curve can be rewritten as $\mu_s c_v$ ($c_v = F_n/v_c$), where c_v is considered the arbitrary damping term to determine at what velocity a line node achieves its kinetic friction force. Once the node velocity becomes large enough to produce a friction force larger than the static friction force, the kinetic friction force is applied.

2.2.1. Normal seabed contact force

In the original MoorDyn formulation [9], the seabed normal contact force on a mooring line node was calculated according to equation (3), where z_b is the depth to the seabed, r_3 is the vertical position of the node, k_b is the seabed stiffness, v_3 is the vertical velocity of the node, c_b is the seabed damping, d is the line segment diameter, and l is the average line segment length on either side of the node:

$$F_n = [(z_b - r_3)k_b - v_3 c_b]dl \tag{3}$$

This equation assumes a general flat seabed where the normal force vector is always vertical. In the new implementation, the seabed can have variable bathymetry, and the seabed normal contact force vector will not always be vertical. To accurately calculate this force, a new seabed normal contact force equation was derived (equation (4)), where $\boldsymbol{v_n}$ is the three-dimensional line node velocity in the normal direction and $\boldsymbol{\hat{n}}$ is the local seabed unit normal vector.

$$\boldsymbol{F_n} = [(z_b - r_3)n_z \boldsymbol{\hat{n}} k_b - \boldsymbol{v_n} c_b]dl \tag{4}$$

The velocity normal to the seabed can now have components in any direction, and the position normal to the seabed can be calculated as the product of the vertical component of position into the seabed ($z_b - r_3$) and the cosine of the angle that the local bathymetry slope makes with the horizontal, which is equal to the vertical component of the seabed unit normal vector (n_z). Now, the seabed normal contact force can have components in the x, y, and z directions, which will be used to calculate friction forces on a line node on any sloped bathymetry.

2.2.2. Friction force directionality
The second critical aspect of the seabed friction implementation is the inclusion of both axial and transverse components of the seabed friction force, where axial motion is along the mooring line's local axis, and transverse motion is perpendicular to its axis. A line node's velocity along the seabed ($\boldsymbol{v}$) can be broken up into axial ($\boldsymbol{v_A}$) and transverse ($\boldsymbol{v_T}$) components as follows,

$$\boldsymbol{v_A} = (\boldsymbol{v} \cdot \boldsymbol{\hat{q}})\boldsymbol{\hat{q}} \tag{5}$$

$$\boldsymbol{v_T} = \boldsymbol{v} - \boldsymbol{v_A} \tag{6}$$

where $\boldsymbol{\hat{q}}$ is the axial unit vector at the node. Using these velocities, the static and kinetic friction force vectors can be calculated in the axial and transverse directions.

$$\boldsymbol{F_{k_T}} = \mu_{k_T}|\boldsymbol{F_n}|\frac{\boldsymbol{v_T}}{|\boldsymbol{v_T}|} \tag{7}$$

$$\boldsymbol{F_{k_A}} = \mu_{k_A}|\boldsymbol{F_n}|\frac{\boldsymbol{v_A}}{|\boldsymbol{v_A}|} \tag{8}$$

$$\boldsymbol{F_{s_T}} = \mu_{s_T}|\boldsymbol{F_n}|\frac{\boldsymbol{v_T}}{|\boldsymbol{v_T}|} \tag{9}$$

$$\boldsymbol{F_{s_A}} = \mu_{s_A}|\boldsymbol{F_n}|\frac{\boldsymbol{v_A}}{|\boldsymbol{v_A}|} \tag{10}$$

Using these equations and the ramp-up considerations of the saturated damping model, the equations for friction force in the axial and transverse directions are shown in the equations ((11)–(13)), with a negative friction force denoting that the friction force acts in the opposite direction of motion:

$$-\boldsymbol{F_{f_T}} = \begin{cases} \boldsymbol{F_{k_T}}, & (\mu_{s_T}c_v)|\boldsymbol{v_T}| > |\boldsymbol{F_{s_T}}| \\ (\mu_{s_T}c_v)\boldsymbol{v_T}, & (\mu_{s_T}c_v)|\boldsymbol{v_T}| < |\boldsymbol{F_{s_T}}| \end{cases} \tag{11}$$

$$-\boldsymbol{F_{f_A}} = \begin{cases} \boldsymbol{F_{k_A}}, & (\mu_{s_A}c_v)|\boldsymbol{v_A}| > |\boldsymbol{F_{s_A}}| \\ (\mu_{s_A}c_v)\boldsymbol{v_A}, & (\mu_{s_A}c_v)|\boldsymbol{v_A}| < |\boldsymbol{F_{s_A}}| \end{cases} \tag{12}$$

$$\boldsymbol{F_f} = \boldsymbol{F_{f_T}} + \boldsymbol{F_{f_A}} \tag{13}$$

The total seabed contact force on each line node ($\boldsymbol{B}$) can then be calculated by summing the friction forces and the normal forces on each line node:

$$\boldsymbol{B} = \boldsymbol{F_f} + \boldsymbol{F_n} \tag{14}$$

Using this methodology, mooring line nodes that rest on the seabed can have the effects of seabed friction and seabed bathymetry factored into their calculations, in both axial and transverse directions, to produce more accurate mooring line simulations in MoorDyn.

3. Verification
To ensure that the previously mentioned seabed features were implemented correctly in MoorDyn, a set of MoorDyn and OpenFAST simulations were run for different mooring systems under various conditions to compare against results from equivalent OrcaFlex simulations. Experimental data for mooring line seabed contact is not easily attainable, and the fact that MoorDyn and OrcaFlex have been validated in other aspects of the code provide a strong enough reason that a verification between the two models is sufficient to confirm the implementation in MoorDyn. The details of each MoorDyn simulation are explained in the first section and the resulting mooring tensions and line kinematics are verified against OrcaFlex results in the second section.

3.1. Model descriptions

The baseline design used to evaluate the effects of these new MoorDyn features is the University of Maine VolturnUS-S semisubmersible platform, which uses the IEA 15 MW reference wind turbine [12]. The mooring system used in the baseline design is a three-line semi-taut mooring system set in a water depth of 850 m off the U.S. West Coast. The mooring system connects to the platform at a fairlead radius of 58 m, it has an anchor radius of 1,130 m, and it includes three semi-taut mooring lines consisting of 500 m of 120-mm R3 Grade studless chain and 1,000 m of 186-mm polyester rope. The design is depicted in Figure 3a.

The baseline design was simulated under a variety of conditions, including wind or waves from three different headings (0°, 60°, 90°) under one of four prescribed seabed bathymetries. The bathymetries include a normal flat bathymetry at an 850-m water depth along with an upslope, a downslope, and a sideslope bathymetry, each at a 12.5% seabed grade ranging from 700 m to 1,000 m of water depth over the mooring footprint. The baseline design was simulated with each of these bathymetries to verify the bathymetry implementation.

To verify the friction implementation, two other models were created to isolate the axial and transverse components of the seabed friction model. The first design used the same mooring system components, but only had Line 1 attached to the fairlead. The model was given a constant platform motion of 0.2 m/s while simulating an anchor failure to model the axial seabed friction effects on the mooring line (Figure 3b). The second design used the same mooring system components as the baseline design, with only Line 1 attached, and was given a constant circular motion of close to 0.9 m/s around an intact anchor to model the transverse seabed friction effects on the mooring line (Figure 3c). The transverse and axial kinetic friction coefficients used in these simulations were 1.0 and 0.69, respectively. In simulations involving the baseline design, the transverse and axial static friction coefficients were 1.33 and 0.92, respectively. In the transverse- and axial-specific simulations, the static friction coefficients were the same as the kinetic coefficients. A saturated damping coefficient (c_v) was set to 10^6 for all simulations based on an earlier sensitivity study.

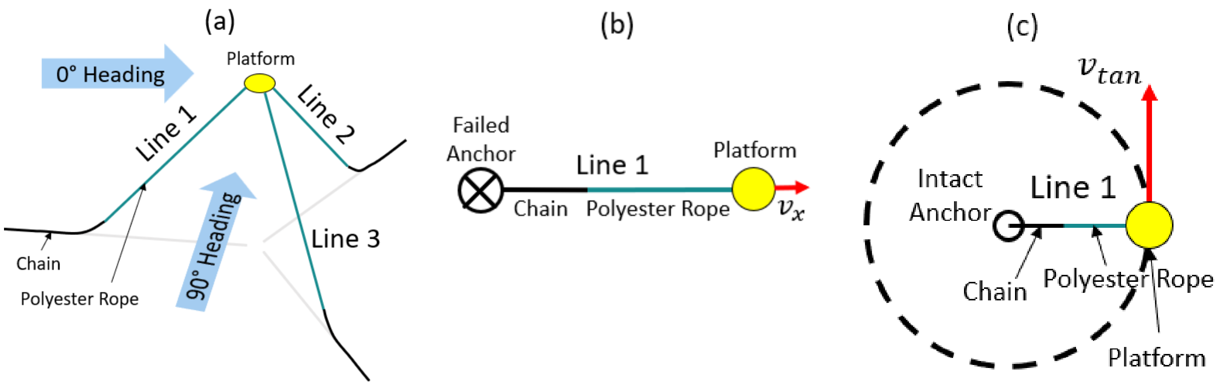

Figure 3. The models used to verify the results from MoorDyn and OrcaFlex. A three-line semi-taut system (a), a one-line system with an anchor failure on Line 1 (b), and a one-line system with prescribed circular motion around an intact anchor (c).

3.2. Bathymetry Verification

The bathymetry feature was modeled in MoorDyn using four different bathymetry layouts: normal, upslope, downslope, and sideslope. Under these four bathymetry grids, the baseline design was run in MoorDyn and OrcaFlex without friction in order to completely isolate the effects from the seabed bathymetry on the mooring system. The fairlead positions from the normal bathymetry case, in response to regular waves with a significant wave height of 9.3 m and a wave period of 14.9 s at a 90° heading, were used to prescribe platform motions for all other bathymetry verifications. A comparison of the fairlead tension of Line 1 between the two models, with depictions of the bathymetry slope, is shown in Figure 4. Only the fairlead tension of Line 1 is shown for conciseness.

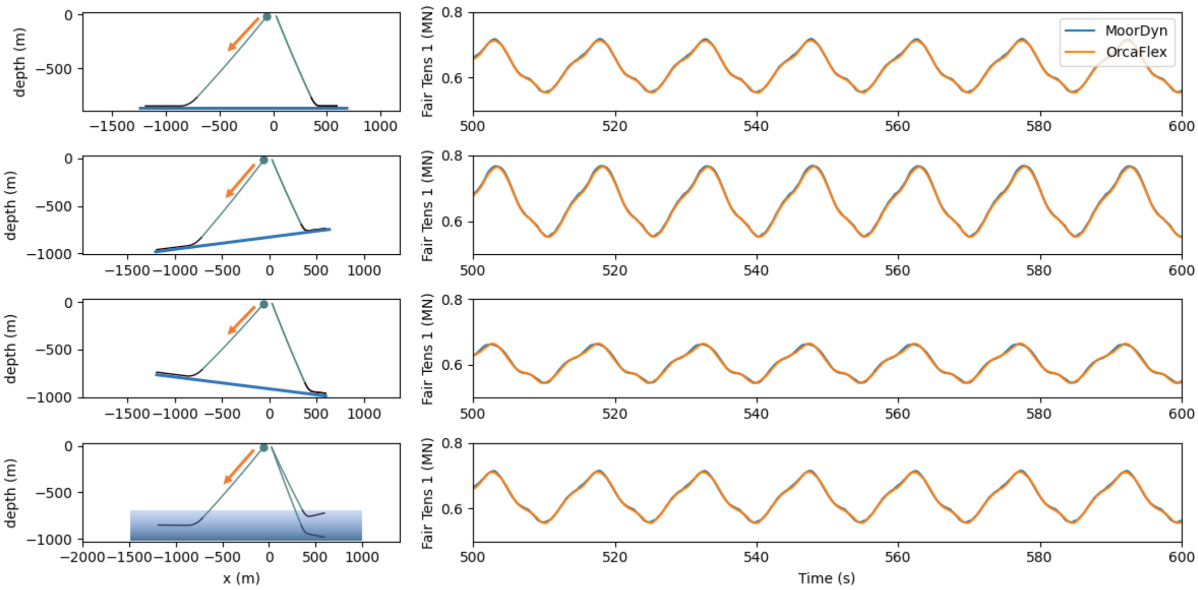

Figure 4. Bathymetry feature verification between MoorDyn (blue) and OrcaFlex (orange) in four different bathymetry grids.

As seen from the fairlead tension time series comparison on the right of Figure 4, the MoorDyn results match very closely with the OrcaFlex results for equivalent simulations, showing that the bathymetry feature was implemented correctly in MoorDyn.

3.3. Friction Verification

The seabed friction feature is verified in three ways. First, the axial friction component of the friction force is isolated by simulating the scenario described in Figure 3b, which prescribes motion in the axial direction. Figure 5 shows the motion of four mooring line nodes on or near the seabed and their x-positions and tensions (which are a function of their attached line segment tensions).

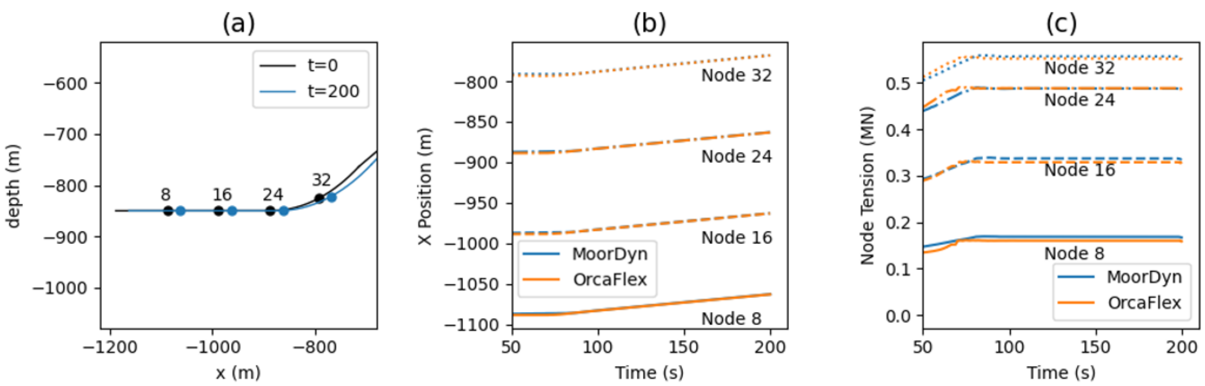

Figure 5. Axial friction component verification results between MoorDyn (blue) and OrcaFlex (orange) with motion of four nodes near the seabed (a), the time series of the x-positions of the four nodes (b), and the time series of the individual node tensions (c).

The x-positions of the four nodes in MoorDyn match very closely with the x-positions of the same nodes in OrcaFlex, and the individual node tensions between the two models vary by less than 5%.

This confirms that MoorDyn accurately models Coulombic friction when a mooring line is sliding freely in the axial direction.

Secondly, the transverse friction component of the friction force is isolated by simulating the scenario described in Figure 3c, which prescribes circular motion around the anchor. Figure 6 shows the motion of the same four mooring line nodes as Figure 5 and their y-positions and tensions.

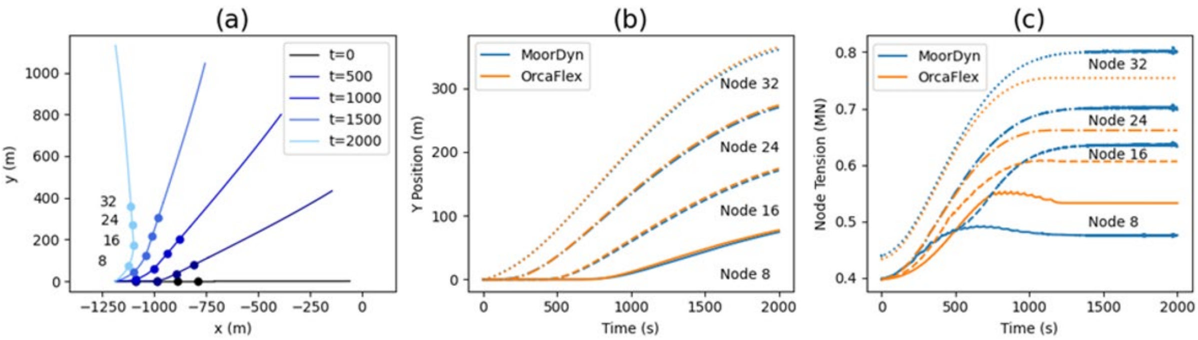

Figure 6. Transverse friction component verification results between MoorDyn (blue) and OrcaFlex (orange) with motion of four nodes near the seabed (a), a time series of the y-positions of the four nodes (b), and a time series of the individual node tensions (c).

The positions of the nodes over time gradually form a curve in the mooring line as it drags transversely along the seabed, proving that there is a transverse seabed friction force resisting the line motion. The y-positions of the four nodes in MoorDyn match very closely with the y-positions of the same nodes in OrcaFlex; however, the individual node tensions between the two models differ by about 5%–15%. The difference in the node tensions is attributed to the difference between the friction model used in MoorDyn and the friction model used in OrcaFlex. MoorDyn's saturated damping friction model calculates friction as a function of line node velocity and allows some sliding at low friction force values. OrcaFlex's friction model calculates friction as a function of line node deflection and keeps nodes stationary until the static friction threshold is overcome. More details on their differences are explained later, but an in-depth analysis is left for future work.

Lastly, the entire friction force was compared and verified by simulating the mooring design described in Figure 3a using steady, 9-m/s wind at a 90° heading, and then using regular waves with a significant wave height of 9.3 m and a wave period of 14.9 s at a 90° heading. Figure 7 shows a comparison of the fairlead tension of Line 1, rather than individual node tensions, between MoorDyn and OrcaFlex under these conditions with friction and without friction.

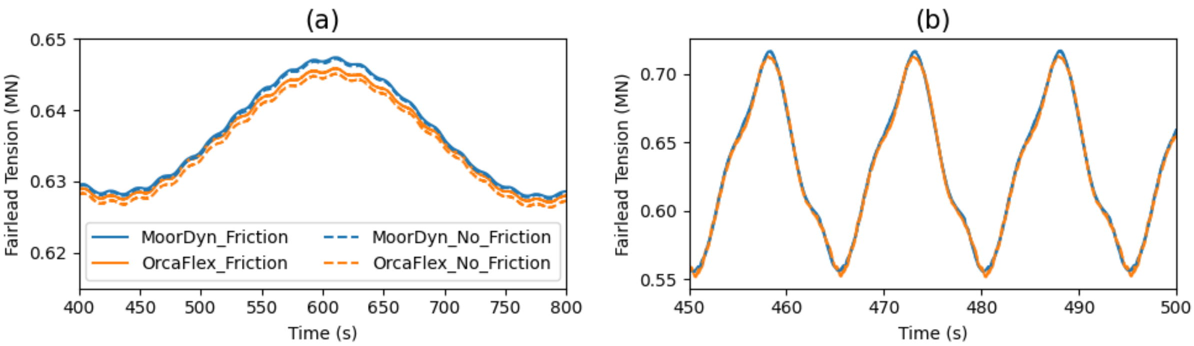

Figure 7. Effect of friction on Line 1 fairlead tensions for the baseline mooring design with wind at a 90° heading (a) and with waves at a 90° heading (b) between MoorDyn (blue) and OrcaFlex (orange).

These simulations are useful for analyzing the differences between static (wind) and dynamic (wave) loading. In Figure 7a, the MoorDyn and OrcaFlex simulations give similar results, but MoorDyn predicts a slightly greater mean fairlead tension while OrcaFlex shows more of a difference between friction and no-friction cases. In Figure 7b, the results are even more aligned, indicating that the friction effects under dynamic wave conditions are less than the friction effects under static wind conditions. In both simulations, the results from MoorDyn and OrcaFlex agree well, which verified the friction implementation, but also shows that the results with and without friction are small, which is likely due to the fact that deep-water mooring systems are not significantly influenced by friction.

A clear example of the differences between the MoorDyn and OrcaFlex friction models appears in the individual Line 1 node tensions on the seabed in the 90° wave heading simulation. Figure 8a shows the time series of node tensions in MoorDyn and Figure 8b shows the time series of node tensions in OrcaFlex. The node tensions calculated in MoorDyn are almost identical across six different nodes, while the node tensions calculated in OrcaFlex decrease as nodes become closer to the anchor.

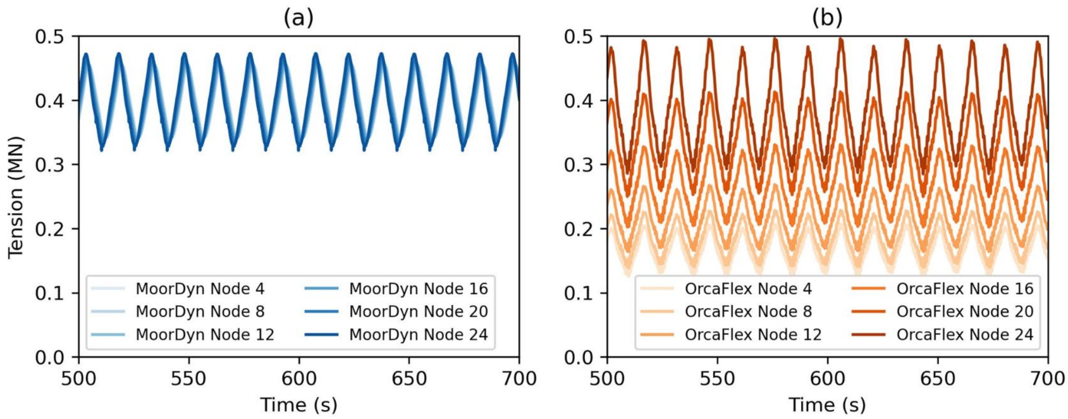

Figure 8. Tensions of nodes on the seabed equilibrate to the same value in MoorDyn (a) and gradually decrease in nodes closer to the anchor in OrcaFlex (b) due to the differences in friction models between the two simulation tools.

This tension difference is a result of a fundamental difference between the MoorDyn and OrcaFlex friction models. In MoorDyn, the nodes are always free to slide and do not experience the full static friction force until they reach a velocity equal to the static friction velocity threshold (v_c in Figure 2b). As a result, the nodes on the seabed will slowly slide to equalize the tensions of the adjacent line segments. In OrcaFlex, the friction model keeps the nodes fully stationary before reaching the friction threshold. The nodes will stay in place at low friction force magnitudes, causing variations in the tension values in different nodes on the seabed. This difference in friction force implementation is also responsible for the different tensions for nodes in the transverse friction isolation case, shown in Figure 6c.

4. Conclusion

Due to the continued development of floating offshore wind energy in areas with more varied seabed conditions, the inclusion of all physical aspects of the mooring system need to be accurately modeled. Seabed bathymetry and seabed friction are now able to be modeled by the open-source mooring dynamics modeler, MoorDyn, that is part of the OpenFAST simulation tool. A seabed bathymetry map of any rectangular discretization can now be imported into a MoorDyn model and used to determine the local seabed depths of line nodes. A saturated damping friction model, which is an altered version of the standard Coulombic friction model that calculates friction force as a function of line node velocity, can calculate the friction force in the axial and transverse directions of the mooring line's heading while accounting for the seabed bathymetry. These features were simulated on a deep-water semisubmersible design in MoorDyn and compared against equivalent OrcaFlex results to verify their accuracy. The MoorDyn results compare well with OrcaFlex, especially for fairlead tensions. Some differences in node tensions along the seabed are a result of the different friction model formulations between the two simulation tools.

A next phase of this verification process would be to compare the differences between more established friction models to evaluate the reliability of each. In conjunction, a study on the differences of friction effects between deep-water and shallow water mooring systems would be of interest, because deep-water mooring systems will generally consist of more semi-taut mooring configurations with less line on the seabed, and shallow-water mooring systems will generally consist of more catenary mooring configurations with more line on the seabed.

Acknowledgement

This work was authored in part by the National Renewable Energy Laboratory, operated by Alliance for Sustainable Energy, LLC, for the U.S. Department of Energy (DOE) under Contract No. DE-AC36-08GO28308. Funding provided by U.S. Department of Energy Office of Energy Efficiency and Renewable Energy Wind Energy Technologies Office for a project led by Principle Power and Awarded by the National Offshore Wind Research and Development Consortium. The views expressed in the article do not necessarily represent the views of the DOE or the U.S. Government. The U.S. Government retains and the publisher, by accepting the article for publication, acknowledges that the U.S. Government retains a nonexclusive, paid-up, irrevocable, worldwide license to publish or reproduce the published form of this work, or allow others to do so, for U.S. Government purposes.

References

[1] ProteusDS | A flexible Dynamic Analysis Tool for Ocean Industries | DSA *DSA Ocean* https://dsaocean.com/proteusds/overview/
[2] OrcaFlex Environment: Seabed data *OrcaFlex Manual Version 11.2b* (Orcina)
[3] Masciola M, Jonkman J and Robertson A 2014 Extending the Capabilities of the Mooring Analysis Program: A Survey of Dynamic Mooring Line Theories for Integration Into FAST *Proc. Int. Conf. on Ocean, Offshore and Arctic Eng.* (San Francisco, California: ASME)
[4] Davidson J and Ringwood J 2017 Mathematical Modelling of Mooring Systems for Wave Energy Converters—A Review *Energies* **10** 46
[5] Azcona J, Nygaard T A, Munduate X and Merino D 2011 Development of a Code for Dynamic Simulation of Mooring Lines in Contact with Seabed *EWEA Offshore* (Amsterdam, The Netherlands)
[6] Lee H-W, Roh M-I, Ham S-H and Ku N-K 2018 Coupled analysis method of a mooring system and a floating crane based on flexible multibody dynamics considering contact with the seabed *Ocean Engineering* **163** 555–569
[7] Choi C-K and Yoo H-H 2012 A dry friction model to realize stick for simulation of the system with friction and accuracy verification of the friction model *Transactions of the Korean Society for Noise and Vibration Engineering* **22** 748–755
[8] Liu Y and Bergdahl L 1997 Influence of current and seabed friction on mooring cable response: comparison between time-domain and frequency-domain analysis *Eng. Struct.* **19** 945–53
[9] Hall M and Goupee A 2015 Validation of a lumped-mass mooring line model with DeepCwind semisubmersible model test data *Ocean Engineering* **104** 590–603
[10] Hall M 2017 Efficient modelling of seabed friction and multi-floater mooring systems in MoorDyn *Proc. 12th European Wave and Tidal Energy Conf.* (Cork, Ireland)
[11] Devries K and Hall M 2018 Comparison of seabed friction formulations in a lumped-mass mooring model *Proc. Int. Offshore Wind Technical Conf.* (San Francisco, California: ASME)
[12] Allen C, Viscelli A, Dagher H, Goupee A, Gaertner E, Abbas N, Hall M and Barter G 2020 *Definition of the UMaine VolturnUS-S Reference Platform Developed for the IEA Wind 15-Megawatt Offshore Reference Wind Turbine* (Golden, Colorado: National Renewable Energy Laboratory)